Military Technical College
Kobry El-Kobbah,
Cairo, Egypt.

17th International Conference on Applied Mechanics and Mechanical Engineering.

ON THE DYNAMICS OF VEHICLE PASSIVE SUSPENSION INCORPORATING TWIN-TUBE PRESSURIZED SHOCK ABSORBER

Y. M. Elattar[1], M. G. Rabie[2] and S. M. Metwalli[3]

ABSTRACT

This paper is dedicated to investigate the dynamic behavior of a typical vehicle passive suspension system. Quarter vehicle suspension with two degree of freedom is presented. A detailed descriptive mathematical model of twin-tube shock absorber was studied. The mathematical model contains the relations of flow rates between the rebound, compression, and reserve chambers. The variable areas of restrictions in both main and bottom valves are also introduced in the mathematical model. The equations describing the system were used to develop a computer simulation program. The shock absorber was tested experimentally using a shock absorber test rig. The simulation and experimental results of the shock absorber dynamic behavior showed good agreement, which validated the developed simulation program. Moreover, the dynamic behavior of a quarter-car model, incorporating the studied shock absorber, was described mathematically, simulated and analyzed.

KEY WORDS

Vehicle passive suspension, Matlab, Simulink, shock absorber, modeling.

[1] Lecturer assistant, Modern Academy for Engineering and Tech., Cairo, Egypt.
[2] Professor of Mech. Engineering, Modern Academy for Engineering and Tech., Cairo, Egypt.
[3] Professor of Mech. Engineering, Faculty for Engineering, Cairo University, Egypt.

NOMENCLATURE

A	Road bump height, (m)
A_{12L}	Equivalent throttling area formed by the orifices in bottom piston valve assembly in L.H.S., (m^2)
A_{12R}	Equivalent throttling area formed by the orifices in bottom piston valve assembly in R.H.S., (m^2)
A_{23L}	Equivalent throttling area formed by the orifices in main piston valve assembly in L.H.S., (m^2)
A_{23R}	Equivalent throttling area formed by the orifices in main piston valve assembly in R.H.S., (m^2)
A_{3H}	Throttling area of three holes on the bottom valve body, (m^2)
A_{6R}	Throttling area of six rectangular holes on the main piston body, (m^2)
A_{7H}	Throttling area of seven holes on the check valve body, (m^2)
A_{8H}	Throttling area of eight holes on the main piston body, (m^2)
A_{8R}	Throttling area of eight rectangular holes on the bottom valve body, (m^2)
A_B	Circumference throttling area formed by negative deflection of the by-pass valve disc, (m^2)
A_C	Circumference throttling area formed by negative deflection of the check valve disc, (m^2)
A_{k1}	Variable circumference throttling area formed by deflection of the rebound valve disc, (m^2)
A_{k2}	Variable circumference throttling area formed by deflection of the compression valve disc, (m^2)
A_{k3}	Variable circumference throttling area formed by deflection of the by-pass valve disc, (m^2)
A_{k4}	Variable circumference throttling area formed by deflection of the check valve disc, (m^2)
A_p	Area of piston, (m^2)
A_{rs}	Area of piston's rod side, (m^2)
A_{t1}	Fixed throttling area on the rebound valve disc, (m^2)
A_{t2}	Fixed throttling area on the compression valve disc, (m^2)
A_{t3}	Fixed throttling area on by-pass valve disc , (m^2)
A_{t4}	Fixed throttling area on check valve disc, (m^2)
B	Oil bulk modulus, (N/m^2)
C_d	Discharge coefficient
C_S	Shock absorber damping ratio
C_{seat}	Seat damping ratio
C_T	Tire damping ratio
D_B	Effective diameter of throttling area formed by negative deflection of by-pass valve disc, (m)
D_C	Effective diameter of throttling area formed by negative deflection of check valve disc, (m)
E	Material Young's modulus, (Pa)
K_S	Spring stiffness, (N/m)
K_{seat}	Seat stiffness, (N/m)
K_T	Tire stiffness, (N/m)
L_{Ak1}	Hydraulic perimeter of the rebound valve disc, (m)
L_{Ak2}	Hydraulic perimeter of the compression valve disc, (m)
L_{Ak3}	Hydraulic perimeter of the by-pass valve disc, (m)
L_{Ak4}	Hydraulic perimeter of the check valve disc, (m)
L_B	Effective hydraulic perimeter for negative deflection of by-pass valve disc, (m)
L_C	Effective hydraulic perimeter for negative deflection of check valve disc, (m)
M_S	Sprung mass, (kg)
M_U	Un-sprung mass, (kg)
P_1	Pressure at reserve chamber, (N/m^2)
P_2	Pressure at compression chamber, (N/m^2)
P_3	Pressure at rebound chamber, (N/m^2)
P_o	Initial charging pressure at reserve chamber, (N/m^2)
Q_1	Total flow rate through the bottom piston valve, from reserve to compression chamber , (m^3/s)
Q_{1L}	Flow rate from reserve chamber to compression chamber through the throttling system A_{12L} (m^3/s)
Q_{1R}	Flow rate from reserve chamber to compression chamber through the throttling system A_{12R} , (m^3/s)

Q_2 Total flow rate through the main piston valve, from compression to rebound chamber , (m^3/s)
Q_{2L} Flow rate from compression chamber to rebound chamber through the throttling system A_{23L} , (m^3/s)
Q_{2R} Flow rate from compression chamber to rebound chamber through the throttling system A_{23R} , (m^3/s)
r_1 Outer contact radius of the rebound valve disc plate, (m)
r_{10} Inner contact radius of shim plates forming the A_B area, (m)
r_{11} Outer contact radius of shim plates forming the A_C area, (m)
r_{12} Inner contact radius of shim plates forming the A_C area, (m)
r_2 Inner contact radius of the rebound valve disc plate, (m)
r_3 Outer contact radius of the compression valve disc plate, (m)
r_4 Inner contact radius of the compression valve disc plate, (m)
r_5 Outer contact radius of the by-pass valve disc plate, (m)
r_6 Inner contact radius of the by-pass valve disc plate, (m)
r_7 Outer contact radius of the check valve disc plate, (m)
r_8 Inner contact radius of the check valve disc plate, (m)
r_9 Outer contact radius of shim plates forming the A_B area, (m)
t_1 Thickness of the rebound valve disc plate, (m)
t_2 Thickness of the compression valve disc plate, (m)
t_3 Thickness of the by-pass valve disc plate, (m)
t_4 Thickness of the check valve disc plate, (m)
t_B Thickness of shim plates forming the A_B area, (m)
t_{be} ending point of bump profile
t_{bs} starting point of bump profile
t_C Thickness of shim plates forming the A_C area, (m)
T_r Rise time,(s)
T_s Settling time, (s)
V_1 Volume of oil at chamber (1), (m^3)
V_2 Volume of oil at chamber (2), (m^3)
V_{2i} Initial volume of oil in chamber (2), (m^3)
V_3 Volume of oil at chamber (3), (m^3)
V_{3i} Initial volume of oil in chamber (3) , (m^3)
V_{Li} Initial volume of compressed oil in rebound chamber, (m^3)
V_o Volume of pressurized gas at pressure P_o, (m^3)
V_T Total volume of rebound chamber, (m^3)
x_1 Displacement of un-sprung mass, (m)
x_2 Displacement of sprung mass, (m)
ρ Oil density, (kg/m^3)
σ Overshoot ratio
ω_b bump width

INTRODUCTION

Passive suspension systems, which consist of conventional elements (springs and dampers), have limitations in controlling the vehicle dynamics. Normal passive suspension parameter choices represent a compromise between the different requirements and the vehicle type and layout [1].

The function of the damper is to dissipate the energy accumulated by the suspension spring displacement. The damping effect is obtained by forcing the oil to flow between

chambers via a set of hydraulic valves, and the damping effect is proficient by the resistance of the oil when moving through these valves [2].

Damping of shock absorber is not the same in rebound and compression strokes. Damping in compression stroke is less than damping in rebound stroke. For that reason, the damping force which is transmitted to the vehicle is less when crossing a road obstacle like a bump. Damping force is greater in rebound stroke to maintain the tire in contact with the road profile as quick as possible. Speed bumps and pot holes are the main cause of vehicle body vibration [3]. MATLAB program has been developed to investigate the dynamic performance of a 2DOF quarter car model.

MATHEMATICAL MODEL OF SHOCK ABSORBER

Mathematical modeling of the valves is introduced in Fig. 1. The model takes into account the nonlinear behavior of the moving parts as well as the variation of throttling areas due to the deflection of circular thin plates. The deflection of the thin circular plate depends on the pressure deference across the plate.

The equations describing the dynamic behavior of the pressurized double tube shock absorber are deduced considering the following assumption [4].

- The density and bulk modulus of the oil are assumed constant.
- The discharge coefficient is constant.
- There is no internal leakage across the piston.
- The main piston is initially in the mid position.
- The gas process is polytropic process (n=1.3).

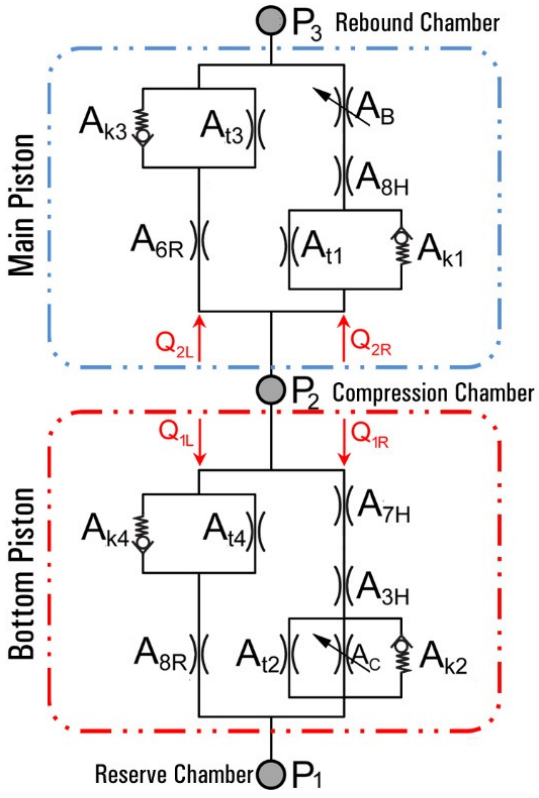

Fig.1. Equivalent scheme for connection of valves and restrictions.

Variation of gas pressure due to oil flow in reserve chamber:

$$\left(P_o + 10^5\right) V_o^{1.3} = \left(P_1 + 10^5\right)\left(V_T - V_1\right)^{1.3} \tag{1}$$

$$V_T = V_{Li} + V_o \tag{2}$$

$$V_1 = V_{Li} - \int (Q_1)dt \tag{3}$$

Flow rate through the main piston valve assembly:

$$Q_2 = Q_{2R} + Q_{2L} \tag{4}$$

$$Q_{2R} = C_d A_{23R}\sqrt{\frac{2}{\rho}(P_2 - P_3)} \tag{5}$$

$$Q_{2L} = C_d A_{23L}\sqrt{\frac{2}{\rho}(P_2 - P_3)} \tag{6}$$

Equivalent throttling area A_{23R} according to pressure difference:

$$A_{23R} = \begin{cases} \sqrt{\left(\dfrac{A_{t1}^2 A_{8H}^2 A_B^2}{A_{8H}^2 A_B^2 + A_{t1}^2 A_B^2 + A_{t1}^2 A_{8H}^2}\right)} & \text{for} \quad P_2 > P_3 \\ \sqrt{\left(\dfrac{\left(A_{k1} + A_{t1}\right)^2 A_{8H}^2 A_B^2}{A_{8H}^2 A_B^2 + \left(A_{k1} + A_{t1}\right)^2 A_B^2 + \left(A_{k1} + A_{t1}\right)^2 A_{8H}^2}\right)} & \text{for} \quad P_2 \le P_3 \end{cases} \tag{7}$$

Variable opening area formed by rebound valve disc [5]:

$$A_{k1} = \begin{cases} L_{Ak1}\dfrac{P_3 - P_2}{E t_1^2}\left(\dfrac{9r_1^4 + 8r_1^3 r_2 - 18r_1^2 r_2^2 + r_2^4}{6 - 4r_1^3 r_2 \ln\left(\dfrac{r_1}{r_2}\right)}\right) & \text{for} \quad P_2 < P_3 \\ 0 & \text{for} \quad P_2 \ge P_3 \end{cases} \tag{8}$$

Circumference throttling area formed by negative deflection of the by-pass valve disc:

$$A_B = \begin{cases} \pi D_B t_B & \text{for} \quad P_2 < P_3 \\ \pi D_B t_B - L_B \dfrac{P_2 - P_3}{E t_5^2}\left(\dfrac{9r_9^4 + 8r_9^3 r_{10} - 18r_9^2 r_{10}^2 + r_{10}^4}{6 - 4r_9^3 r_{10} \ln\left(\dfrac{r_9}{r_{10}}\right)}\right) & \text{for} \quad P_2 \ge P_3 \end{cases} \tag{9}$$

Equivalent throttling area A_{23L} according to pressure difference:

$$A_{23L} = \begin{cases} \sqrt{\left(\dfrac{(A_{k3} + A_{t3})^2 A_{6R}^2}{(A_{k3} + A_{t3})^2 + A_{6R}^2} \right)} & \text{for} \quad P_2 > P_3 \\ \sqrt{\left(\dfrac{A_{t3}^2 A_{6R}^2}{A_{t3}^2 + A_{6R}^2} \right)} & \text{for} \quad P_2 \le P_3 \end{cases} \tag{10}$$

Variable opening area formed by by-pass valve disc:

$$A_{k3} = \begin{cases} 0 & \text{for} \quad P_2 < P_3 \\ L_{Ak3} \dfrac{P_2 - P_3}{E t_3^2} \left(\dfrac{9r_5^4 + 8r_5^3 r_6 - 18 r_5^2 r_6^2 + r_6^4}{6 - 4 r_5^3 r_6 \ln\left(\dfrac{r_5}{r_6} \right)} \right) & \text{for} \quad P_2 \ge P_3 \end{cases} \tag{11}$$

Flow rate through the bottom piston valve assembly:

$$Q_1 = Q_{1R} + Q_{1L} \tag{12}$$

$$Q_{1R} = C_d A_{12R} \sqrt{\frac{2}{\rho}(P_2 - P_1)} \tag{13}$$

$$Q_{1L} = C_d A_{12L} \sqrt{\frac{2}{\rho}(P_2 - P_1)} \tag{14}$$

Equivalent throttling area A_{12R} according to pressure difference:

$$A_{12R} = \begin{cases} \sqrt{\left(\dfrac{(A_{t2} + A_C)^2 A_{3H}^2 A_{7H}^2}{A_{3H}^2 A_{7H}^2 + (A_{t2} + A_C)^2 A_{7H}^2 + (A_{t2} + A_C)^2 A_{3H}^2} \right)} & \text{for} \quad P_1 > P \\ \sqrt{\left(\dfrac{(A_{k2} + A_{t2} + A_C)^2 A_{3H}^2 A_{7H}^2}{A_{3H}^2 A_{7H}^2 + (A_{k2} + A_{t2} + A_C)^2 A_{7H}^2 + (A_{k2} + A_{t2} + A_C)^2 A_{3H}^2} \right)} & \text{for} \quad P_1 \le P \end{cases} \tag{15}$$

Variable opening area formed by compression valve disc:

$$A_{k2} = \begin{cases} L_{Ak2} \dfrac{P_2 - P_1}{E t_2^2} \left(\dfrac{9r_3^4 + 8r_3^3 r_4 - 18 r_3^2 r_4^2 + r_4^4}{6 - 4 r_3^3 r_4 \ln\left(\dfrac{r_3}{r_4} \right)} \right) & \text{for} \quad P_2 > P_1 \\ 0 & \text{for} \quad P_2 \le P_1 \end{cases} \tag{16}$$

Circumference throttling area formed by negative deflection of the check valve disc:

$$A_C = \begin{cases} \pi D_C t_C & \text{for} \quad P_1 < P_2 \\ \pi D_C t_C - L_C \dfrac{P_1 - P_2}{E t_C^2} \left(\dfrac{9r_{11}^4 + 8r_{11}^3 r_{12} - 18 r_{11}^2 r_{12}^2 + r_{12}^4}{6 - 4 r_{11}^3 r_{12} \ln\left(\dfrac{r_{11}}{r_{12}}\right)} \right) & \text{for} \quad P_1 \geq P_2 \end{cases} \quad (17)$$

Equivalent throttling area A_{12L} according to pressure difference:

$$A_{12L} = \begin{cases} \sqrt{\left(\dfrac{(A_{k4} + A_{t4})^2 A_{8R}^2}{(A_{k4} + A_{t4})^2 + A_{8R}^2} \right)} & \text{for} \quad P_1 > P_2 \\ \sqrt{\left(\dfrac{A_{t4}^2 A_{8R}^2}{A_{t4}^2 + A_{8R}^2} \right)} & \text{for} \quad P_1 \leq P_2 \end{cases} \quad (18)$$

Variable opening area formed by check valve disc:

$$A_{k4} = \begin{cases} \sqrt{\left(\dfrac{(A_{k4} + A_{t4})^2 A_{8R}^2}{(A_{k4} + A_{t4})^2 + A_{8R}^2} \right)} & \text{for} \quad P_2 > P_1 \\ L_{Ak4} \dfrac{P_1 - P_2}{E t_4^2} \left(\dfrac{9r_7^4 + 8r_7^3 r_8 - 18 r_7^2 r_8^2 + r_8^4}{6 - 4 r_7^3 r_8 \ln\left(\dfrac{r_7}{r_8}\right)} \right) & \text{for} \quad P_2 \leq P_1 \end{cases} \quad (19)$$

Continuity equation for chamber compression chamber (2):

$$A_p \frac{dx}{dt} + Q_1 - Q_2 = \frac{V_2}{B} \frac{dP_2}{dt} \quad (20)$$

where the term $[V_2 / B] / [dP_2 / dt]$ is the effect of the compressibility at the compression chamber (2).

$$V_2 = V_{2i} - A_p x \quad (21)$$

Continuity equation for chamber compression chamber (3):

$$Q_1 - A_{rs} \frac{dx}{dt} = \frac{V_3}{B} \frac{dP_3}{dt} \quad (22)$$

where the term $[V_3/B]/[dP_3/dt]$ is the effect of the compressibility at the rebound chamber (3).

$$V_3 = V_{3i} + A_{rs}x \tag{23}$$

COMPUTER SIMULATION OF SHOCK ABSORBER

The studied shock absorber was described mathematically by equations 1 thru 23. These equations were used to develop a MATLAB™ Simulink® simulation program. The constants data including dimensions were determined by direct measurements of the elements of a disassembled shock absorber.

EXPERIMENTAL SETUP

In order to validate the developed simulation program, shock absorber should be tested experimentally with a test rig. So the studied shock absorber was tested on MTS-850 test rig (Fig. 2) in the Technical Research Center. This test rig consists of four main parts, load unit, hydraulic power supply, digital controller, and a PC. Shock absorber is subjected to sinusoidal input of amplitude 100 mm and six different frequencies starting from 1Hz to 6Hz. These range of low frequencies applied because if the shock absorber operated at higher frequency, the higher internal pressures cause blow-off valves to open. The characteristic diagram shows a break point where these pressure controlled valves open. For higher frequencies the amount of hysteresis increases. It is clear that different characteristic diagrams can be observed for different excitations [6, 7].

Fig. 2. MTS-850 test rig.

SHOCK ABSORBER MODEL VALIDATION

Validation of the simulation program was evaluated by comparing both theoretical and experimental results. The purpose of this validation is to investigate how far the developed computer program is descriptive to the real.

Both of theoretical and experimental generated damping forces are shown in (Fig.3) to (Fig. 6). These figures show a good agreement between both theoretical and experimental results. Figures (5) and (6) show that the damping coefficient C_S is higher in rebound stroke than its value in compression stroke.

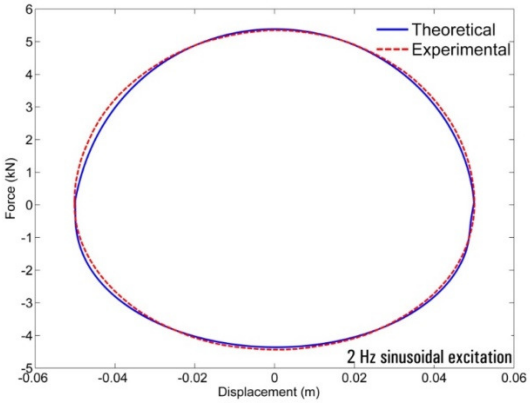

Fig.3. Generated damping force with displacement due to a sinusoidal input of 2 Hz frequency and constant amplitude of 100 mm.

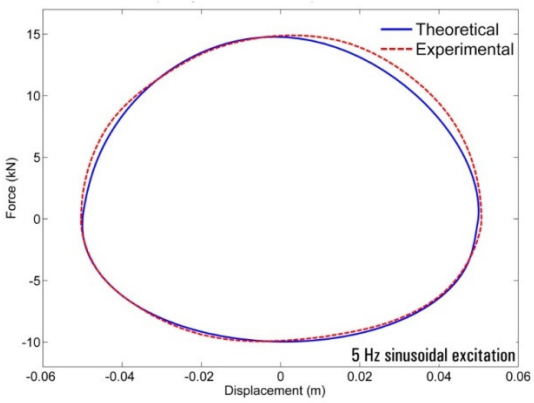

Fig.4. Generated damping force with displacement due to a sinusoidal input of 5 Hz frequency and constant amplitude of 100 mm.

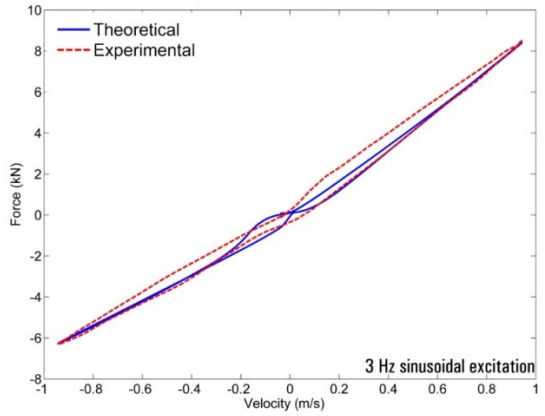

Fig.5. Generated damping force with velocity due to a sinusoidal input of 3 Hz frequency and constant amplitude of 100 mm.

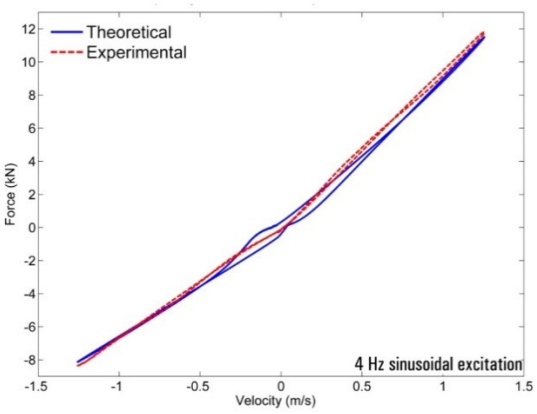

Fig.6. Generated damping force with velocity due to a sinusoidal input of 4 Hz frequency and constant amplitude of 100 mm.

QUARTER VEHICLE MATHEMATICAL MODEL

Two degrees of freedom vehicle model for sprung and un-sprung mass is constructed and its dynamic characteristics are investigated theoretically. The two degree of freedom model shown in (Fig. 7) includes an un-sprung mass representing the wheels and associated components (M_U) and a sprung mass representing the vehicle body (M_S). Their motion in the vertical direction can be described by two coordinates, x_1 and x_2, with origins at the static equilibrium positions of the un-sprung and sprung masses, respectively. This model can be used to represent a quarter of a vehicle. By applying Newton's second low to the sprung and un-sprung masses separately, the equations of motion of the system can be obtained. For vibration excited by surface undulation, the equations of motion are as follows:

$$M_S\ddot{x}_2 + C_S(\dot{x}_2 - \dot{x}_1) + k_S(x_2 - x_1) = 0 \tag{24}$$

$$M_U\ddot{x}_1 + C_S(\dot{x}_1 - \dot{x}_2) + k_S(x_1 - x_2) + C_T\dot{x}_1 + k_T x_1 = -f(t) \tag{25}$$

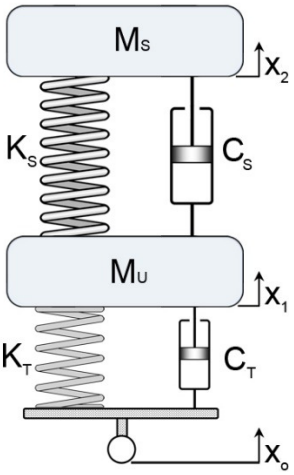

Fig.7. Quarter vehicle model utilizing passive suspension.

Table 1. Quarter vehilce model parameters for studied vehicle utilizing passive suspension.

Parameter	Value
M_S	236 kg
M_U	28.5 kg
K_S	16 kN/m
K_T	180 kN/m
C_T	13.2 N/m

$$f(t) = -C_T\dot{x}_o - k_T x_o \tag{26}$$

In order to simulate the suspension response of the studied vehicle, all the data in (Table 1) is gathered either by physical measuring or by obtaining form the manufacturer's catalogue.

STEP ROAD PROFILE MODELING

Metwalli et al., [8] presented a technique facilitated the use of deterministic numerical simulation results or direct solutions without working with the difficult frequency domain integrals. A sample application is presented to demonstrate that a step input can be equivalent to a hyperbolic spectral density. A linear system is subjected to the hyperbolic spectral density and the equivalent step. The calculated root mean square outputs are found to be identical. Deterministic equivalents for other random signals are also indicated.

RMS values of the outputs of the step input applied to a fourth order system are found to be exactly identical to those for the hyperbolic spectral density input. Different first, second, third and fourth order systems have been examined. These systems have been subjected to hyperbolic, white noise displacement and acceleration spectral densities and the Poisson process in the random domain. The same systems have been subjected respectively to step, impulse, ramp, and exponential functions as time equivalents. The RMS results obtained for different outputs for a random input were identical to those obtained for the equivalent time input [9]. This was true for all systems considered. Hence, these results validate the applicability of the transform to linear systems.

ROAD BUMP OBSTACLE PROFILE MODELING

A road bump was implemented to investigate the dynamics of the quarter vehicle crossing over it. Equation 27 describes the vertical velocity of vehicle exposed to the road bump. The bump parameters are determined in (Table 2). Fig. 8 shows the road bump obstacle simulation which was described by (equation 27).

$$\frac{dx_o}{dt}(t) = \begin{cases} A\omega_b \cos\omega_b t & \text{for} \quad t_{bs} \le t \le t_{be} \\ 0 & \text{for} \quad \text{otherwise} \end{cases} \tag{27}$$

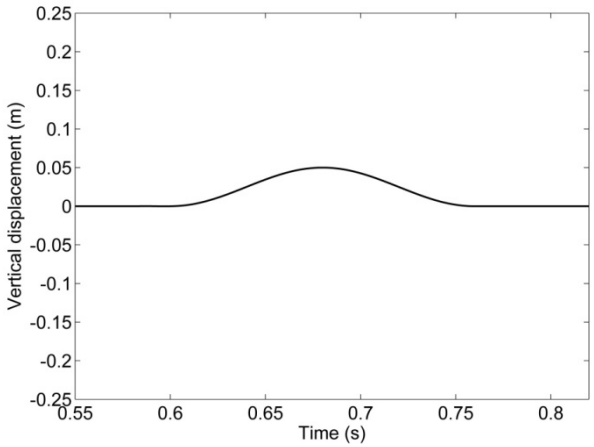

Fig.8. Generated road bump described by equation 27.

Table 2. Road bump parameters.

Parameter	Value
Bump height	0.05 m
Bump width	0.2 m
Vehicle velocity	2.5 m/s

SIMULATION OF QUARTER VEHICLE UTILIZING PASSIVE SUSPENSION

Equations (24) to (26) are describing the quarter vehicle model utilizing a typical passive suspension system with the parameters in (Table 1). The dynamic behavior of the vehicle was investigated theoretically by the exploitation of these equations, using MATLAB™ Simulink® software. The model contains the sprung mass, un-sprung mass, tire stiffness, tire damping, suspension spring stiffness, and the detailed model of shock absorber which was developed previously.

DYNAMIC RESPONSE OF PASSIVE SUSPENSION

The simulation program can predict the transient response of the quarter vehicle model equipped with the studied shock absorber for road profile input.

RESULTS AND DISCUSSION

Two different road profiles are used to simulate the input for the quarter vehicle. It is necessary also to discuss the modeling of the road bump obstacle. The responses are calculated for the following road profiles:

- Step road obstacle.
- Road bump obstacle.

Response of Due to Step Road Obstacle

The calculation results are plotted in (Fig. 9). This figure shows that the sprung mass has a settling time of 1.28 s and maximum percentage overshoot of 48%. The unsprung mass response shows that it has a settling time of 0.31 s and maximum percentage overshoot of 20%.

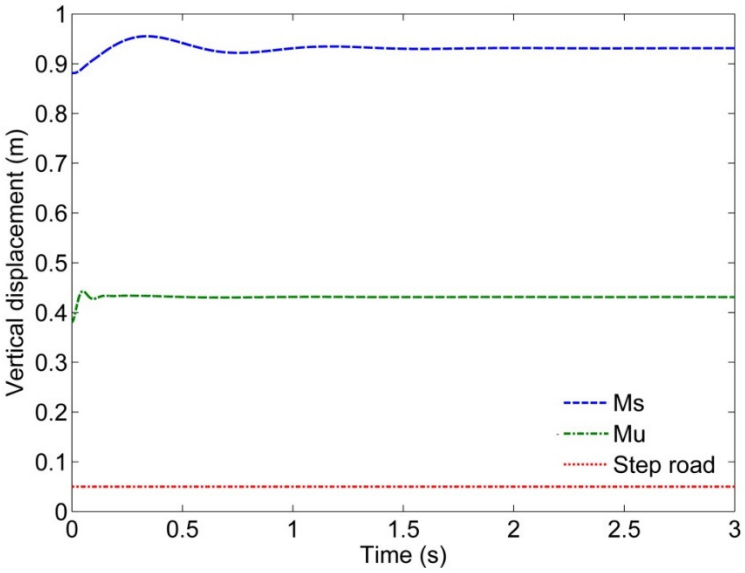

Fig. 9. Response of sprung and unsprung masses due to step road of 5 cm.

Response of Due to Road Bump Obstacle

The dynamic response of the sprung and unsprung masses of a vehicle equipped with passive suspension due to road bump input is shown in (Fig. 10). The vehicle was moving with a speed of 2.5 m/s.

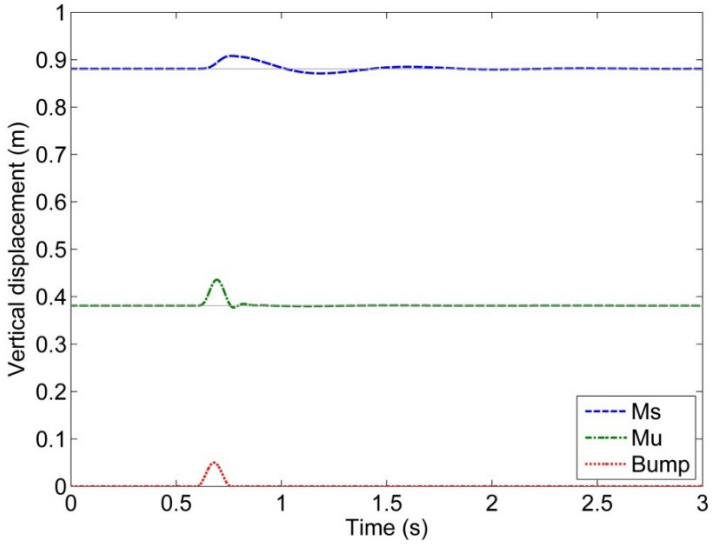

Fig. 10. Transient response of masses due to road bump.

The transient response of the unsprung mass due to the road obstacle is shown in (Fig. 11). This figure shows that the unsprung mass response is following the obstacle profile with 10% increase in magnitude and -11.25° in phase shift. Fig. 12 shows the transient response of the sprung mass. It is noticed that the maximum sprung mass displacement within only 2 cm which is 40% the bump height.

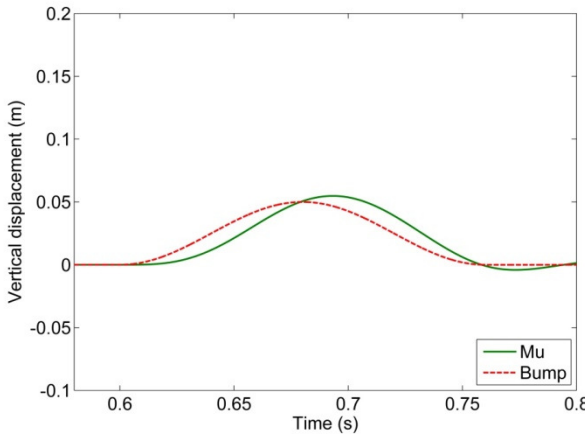

Fig. 11. Unsprung mass (Mu) dynamic response due to road bump input.

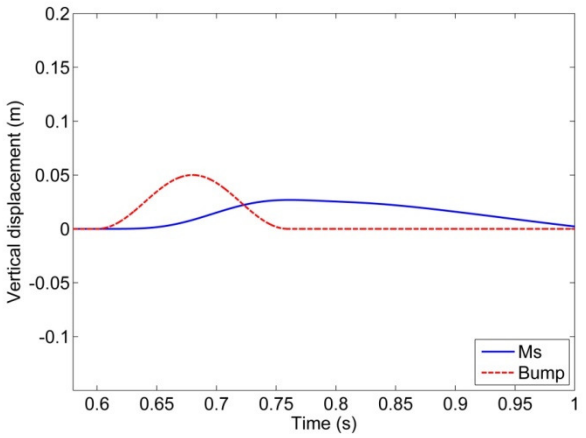

Fig. 12. Unsprung mass (Ms) dynamic response due to road bump input.

SUMMARY OF RESULTS

Results obtained from each of mathematical and experimental study of the double tube shock absorber are summarized as following:

1. The damping coefficient of the studied twin-tube shock absorber in the rebound stroke is higher than the damping coefficient in the compression stroke.
2. Maximum forces in the rebound and compression stroke were found at the middle of piston stroke which corresponding to the maximum piston speed in the case of using input displacement in the form of sinusoidal road.
3. In the force displacement relation, the area under the curve determines the work done by the shock absorber which indicates the energy dissipated. It is found that the energy dissipated increases with the increase of the frequency (velocity) and the increase of stroke displacement.
4. It was found that the force-velocity relation is nonlinear, during the rebound and the compression strokes. Consequently, the damping coefficient is not constant. It changes during the working stroke.
5. The constant rate characteristics of the shock absorber, which means that the generated damping force depends only on the velocity across the SA, should be controlled to give the optimum ride and handling characteristics.
6. It was found that the arrangements of the throttling areas and the variation of these areas, in the rebound and compression valves, play the main roll to perform the required damping in the suspension.
7. For a step road obstacle, the sprung mass showed a settling time of 1.28 s and maximum percentage overshoot of 48%. The unsprung mass showed a settling time of 0.31 s and maximum percentage overshoot of 20%.
8. For the typical road bump obstacle, the response of the unsprung mass showed that it is following the road obstacle profile with 10% increase in magnitude and -

11.25° in phase shift. While the sprung mass showed a maximum displacement within only 2 cm, which is 40%, the bump height.

CONCLUSION AND FUTURE WORK

The dynamic behavior of a twin-tube-pressurized shock absorber is investigated experimentally and theoretically. The theoretical study consisted of the deduction of a mathematical model with special attention to the shock absorber variable area restrictions. The good agreement between the experimental and theoretical results validated the simulation program.

The dynamic behavior of a quarter car, incorporating the studied shock absorber was investigated. Considering a typical road obstacle the quarter car showed an underdamped transient response of 1.28 s settling time, 48% over shoot and 7.2 rad/s natural frequency.

The developed and validated simulation program is convenient for future investigation of car dynamics considering diverse shapes of road obstacles and vehicle speed keeping an eye on the passengers comfort.

REFERENCES

[1] Dixon C. J., 2007, “The Shock Absorber Handbook”, John Wiley & Sons Ltd, England.
[2] Subramanian, Shanmugasundaram, R. Surampudi, and K. R. Thomson, 2003, Development of a nonlinear shock absorber model for low-frequency applications. No. 2003-01-0860. SAE Technical Paper.
[3] Sharma P., Nittin S., Dimple S., and Parveen S., 2013, "Analysis of Automotive Passive Suspension System with Matlab Program Generation. "International Journal of Advancements in Technology 4, pp. 115-119.
[4] Ziad A. I., 2006, “Design and Analysis of Active Vehicle Suspension Systems”, PhD. Thesis, Military Technical College, Cairo, Egypt.
[5] Yuming H., Lingyang L., Ping H., Yunqing Z., and Liping C., 2011, “Shock Absorber Modeling and Simulation Based on Modelica”, Proceedings 8th Modelica Conference, Dresden, Germany, pp. 843-846.
[6] Duym, Stefaan, Randy S., and Koenraad R., 1997, "Evaluation of shock absorber models." Vehicle system dynamics 27, no. 2, pp. 109-127.
[7] Lu, Y. J., S. H. Li, and Na C., 2013, "Research on damping characteristics of shock absorber for heavy vehicle." Research Journal of Applied Science, Engineering and Technology 5, no. 3, pp. 842-7.
[8] Ghoneim, H., Metwalli S. M., 1984, “Optimum Vehicle Suspension with a Damped Absorber.” Journal of Mechanical Design 106, No. 2, pp. 148-155.
[9] Metwalli S. M., Mayne, R. W. , 1981, “Random to deterministic transform”, Journal of sound and vibration 79, no. 2, 1981, pp. 197-204.